

# **DYNAMICS ASPECTS OF PLUTONIUM RECYCLING IN PWRs: INFLUENCE OF THE MODERATOR-TO-FUEL RATIO**

Jan Leen Kloosterman  
Delft University of Technology  
Interfaculty Reactor Institute (IRI)  
Mekelweg 15  
NL-2629 JB Delft, Netherlands  
E-mail: J.L.Kloosterman@iri.tudelft.nl

## **ABSTRACT**

The dynamic behaviour of MOX fuelled PWRs with moderator-to-fuel (MF) ratio between two and four is compared with that of a standard UO<sub>2</sub> fuelled PWR with MF=2. Three different methods have been used: linear stability analysis, quasi-stationary analysis, and numerical analysis. From the first method it can be concluded that for a MOX-fuelled reactor to behave like an UO<sub>2</sub>-fuelled one, the MF ratio should be three for plutonium during the first recycling, and about four for plutonium after four times recycling.

From the other two methods it can be concluded that for transients leading to an instantaneous increase of the reactivity, an MF ratio of 2.5 has preference, due to the relatively stronger negative fuel and moderator temperature coefficients (stronger when expressed in units of  $\beta_{eff}$ ). When the coolant flow rate decreases, the same MF ratio has preference, while an MF ratio of four should be used when the flow rate increases. The ratio of power and flow rate is rather insensitive to the MF ratio used. When the inlet temperature of the coolant decreases, a large MF ratio of four should be used for recycling plutonium containing a large fraction of fissile isotopes, while an MF ratio of two has preference when recycling degraded plutonium.

## **1. INTRODUCTION**

With the increasing interest to use plutonium as a fuel in Pressurized Water Reactors (PWRs), many papers have been published on mainly two subjects: Compatibility of MOX

fuel assemblies with assemblies containing only  $\text{UO}_2$  fuel, and the influence of (multiple) recycling of plutonium on spent fuel characteristics like radiotoxicity, heat production, and neutron and gamma emission.

Examples of the first category mostly focus on the pin power distribution within MOX assemblies, on the power distribution in the MOX fuel areas surrounded by  $\text{UO}_2$  fuel, on the reactivity of the MOX assemblies as a function of burnup, and on (preliminary) transient analysis. Typically, a MOX fuel assembly consists of three zones containing different plutonium weight fractions to flatten the power profile. The MOX fuel fraction in the core typically ranges from 30 to 50%. Reference 1 provides an overview of design criteria, licensing issues and core characteristics of reactors partly fuelled with MOX assemblies. Many more references can be found in proceedings of recent GLOBAL, ENC, and PHYSOR conferences. Studies and experience in fabrication and irradiation of MOX fuel trend towards higher burnup<sup>2</sup> and a larger MOX fraction in the core with final goal a full MOX core with exit burnup of about 65 GWd/tHM. A first investigation on the control feasibility of a full MOX core was published already in 1990<sup>3</sup>, which showed the need for high-density absorber rods enriched up to 90% in the isotope  $^{10}\text{B}$ . A more complete design of a full MOX reactor is presented in Ref. 4. Besides using enriched boron, the moderator-to-fuel ratio was enlarged to increase the reactivity worth of the soluble boron and of the control rods. No intra-assembly plutonium content zoning is necessary in this case, because of the homogeneous core composition. Besides assembly and core design, attention is paid to control and accidental behaviour of the reactor. Again, other feasibility studies on full MOX cores can be found in proceedings of recent GLOBAL, ENC, and PHYSOR conferences. Finally, the use of inert matrices should be mentioned. Many experimental and calculation studies aim at the use of uranium-free plutonium fuels in thermal reactors to enhance the net plutonium consumption. A neutronic and thermal-hydraulic design of an advanced annular fuel concept is presented in Ref. 5. The assembly in this case consists of 36 annular fuel rods containing  $\text{PuO}_2$  mixed in  $\text{CeO}_2$  and 120 standard  $\text{UO}_2$  rods, enabling the designer to meet the design requirements of the core and to have a very high local moderator-to-fuel volume ratio of six. A comparison of core characteristics like power peaking, reactivity coefficients, and shutdown margin between a full MOX core and a uranium-free core, as well as considerations about transient behaviour are given in Ref. 6. Also here, the uranium-free fuel has an annular geometry to reduce the maximum temperature in the fuel.

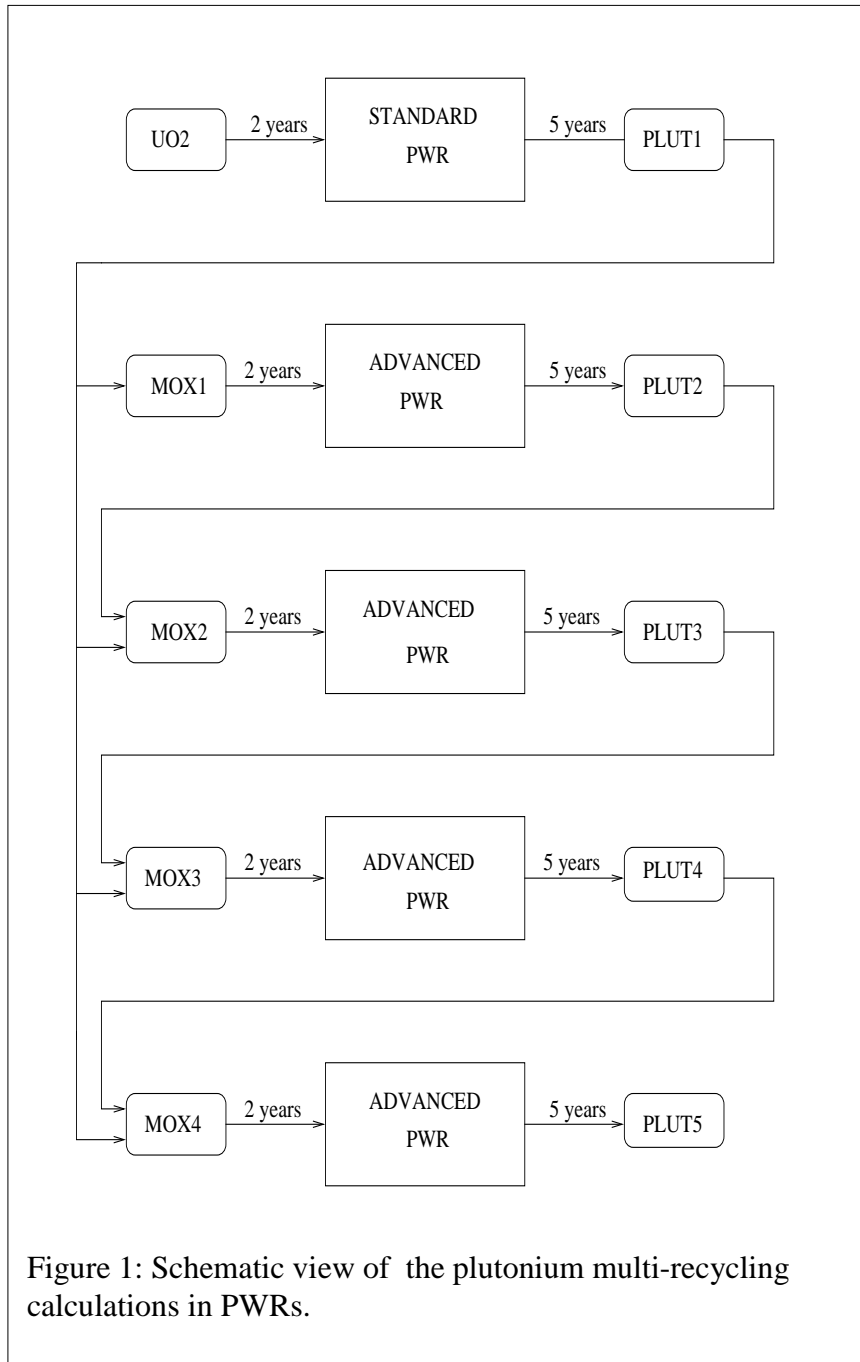
An example of the second category of papers is given in Ref. 7 that addresses the characteristics of spent MOX fuel with burnup as a parameter (40-55 GWd/tHM), and the influence of multi-recycling of self-generated plutonium on these characteristics. Results of the multi-recycling calculations with burnup of 50 GWd/tHM are compared with those of low-burnup MOX fuels (33 GW/tHM). Many more publications on this topic can be found in proceedings of recent GLOBAL and ENC conferences, for example.

Besides these two categories of papers, only few papers address the issue of reactor *dynamics* associated with the use of plutonium as a fuel. Of course, each innovative fuel design needs its own analysis that usually consists of calculating the necessary reactivity coefficients and kinetic parameters, in many cases followed by a preliminary analysis of some selected transients<sup>4,6</sup>. Only a recent paper addresses the transient behavior of MOX fuel,

specifically for the class of cooling accidents that seems to be the most penalising one for the use of MOX fuel<sup>8</sup>. A more rigorous approach to reactor dynamics of a non-homogeneous reactor is given in Ref. 9 that presents a treatment to calculate the best position of a pure uranium shell in a plutonium fuelled core in order to improve the dynamic response of the reactor. In reverse way, it presents the worst position of a plutonium shell in a uranium fuelled core. The better reactor is defined as the one with the smaller fundamental time eigenvalue.

This paper's aim is to present a systematic approach to reactor dynamics associated with multiple recycling of self-generated plutonium in PWRs with the moderator-to-fuel volume ratio (in the remainder of this article referred to as the "MF ratio") as a parameter. Results focus on trends, rather than on accurate results. Three methods are applied: Linear stability analysis (Section three), Quasi-static analysis (Section four), and Numerical analysis in Section five. The first method is used to investigate the behaviour of the reactor upon small reactivity disturbances, the second method to investigate the stationary values of parameters like power and/or temperatures after specific transients, while the last method gives information of these parameters during the transients.

Input parameters of the study presented here are based on one-dimensional calculations with the OCTOPUS burnup and criticality code system<sup>10</sup>. A detailed description of these calculations is given in literature<sup>11,12</sup>, so here only a short outline of the recycling procedure will be presented. Plutonium generated in a UO<sub>2</sub>-fuelled PWR with exit burnup of 47.5 GWd/tHM is assumed to be stored for five years, reprocessed and subsequently used for the manufacturing of MOX fuel assuming a fabrication throughput time of two years. Subsequently, this MOX fuel is irradiated in a PWR with a specific MF ratio between two and four after which the spent MOX fuel is stored for five years and reprocessed. The plutonium thus obtained is mixed with plutonium in spent UOX fuel with a blending ratio of three (this means that the spent MOX fuel is reprocessed together with a three times larger amount of spent UO<sub>2</sub> fuel), and used to fabricate new MOX fuel for the next recycling stage. This recycling process has been repeated four times. A schematic view of the whole recycling procedure is shown in Fig. 1. Although in the calculations the MF ratio has been varied by either reducing the fuel pin radius or by increasing the fuel rod pitch, in this paper only the results of the first method are used, as this is the most realistic one to increase the MF ratio. To keep constant the heat flux at the rod outer boundary, the linear power is taken proportional to the fuel pin radius, which means that the power density is proportional to the inverse of the radius. The weight fraction of plutonium in the MOX fuel at each recycling stage is calculated such that the exit burnup of the MOX fuel equals that of the UO<sub>2</sub> fuel (47.5 GWd/tHM). The concentration of the soluble boron at beginning of each fuel cycle is such that the reactivity gain due to the linearly decreasing boron concentration compensates for the reactivity loss due to burnup. The fuel and moderator reactivity coefficients and the kinetic parameters like the effective delayed neutron fractions, the associated neutron precursor decay-time constants, and the neutron generation time are averaged over burnup. The results of all these elaborate calculations are reactivity coefficients and kinetic parameters for MOX fuelled PWRs with an MF ratio between two and four containing either once, two, three or four times recycled plutonium.



## 2. REACTOR MODEL

In this section, a point-kinetics reactor model is described with fuel and moderator temperature feedback mechanisms. In the model, all reactivity coefficients, kinetic parameters, heat capacities, and heat-transfer coefficients are assumed constant and

independent of the actual fuel and moderator temperatures. The equations for the thermal power density  $P$  and the concentration of the delayed neutron precursors  $D_i$  are given by<sup>13</sup>:

$$\frac{dP}{dt} = \frac{\rho(t) - \beta}{\Lambda} P(t) + \sum_{i=1}^6 \lambda_i D_i(t),$$

and:

$$\frac{dD_i}{dt} = \frac{\beta_i}{\Lambda} P(t) - \lambda_i D_i(t) \text{ for } i = 1..6$$
(1)

Here  $\rho$  is the reactivity,  $\beta$  is the sum of six delayed neutron fractions  $\beta_i$ ,  $\lambda_i$  are the associated neutron precursor decay time constants, and  $\Lambda$  is the neutron generation time. The  $D_i$  is the delayed neutron precursor concentration for group  $i$  expressed in latent heat.

The fuel and moderator temperatures are described by two ‘lumped-parameter’ equations<sup>14</sup>:

$$\frac{dT_f}{dt} = \frac{1}{C_f} P(t) - \gamma_f (T_f - T_m),$$

and:

$$\frac{dT_m}{dt} = \gamma_m (T_f - T_m) - h_m (T_{out} - T_{in}).$$
(2)

Here  $\gamma_f$  and  $\gamma_m$  are the inverse time constants of the fuel and moderator, respectively, given by:

$$\gamma_f = \frac{h_s A_f}{C_f} \text{ and } \gamma_m = \frac{h_s A_m}{C_m}$$
(3)

where  $C_f$  and  $C_m$  are the heat capacities of the fuel and moderator, respectively ( $\text{J cm}^{-3} \text{K}^{-1}$ ), and  $A_f$  and  $A_m$  are the contact surfaces between fuel and moderator per unit volume of the fuel ( $A_f$ ) and per unit volume of the moderator ( $A_m$ ). The heat-transfer coefficient is given by  $h_s$  ( $\text{W K}^{-1} \text{cm}^{-2}$ ). Note that with increasing MF ratio, both the power density and  $\gamma_f$  are proportional to the inverse of the fuel pin radius, which means that the fuel and moderator temperatures do not change from one fuel design to the other.

Substituting the initial boundary conditions:

$$\frac{dT_f(0)}{dt} = 0 \text{ and } \frac{dT_m(0)}{dt} = 0$$
(4)

in Eqs. (2) gives:

$$h_s = \frac{P(0)}{A_f} \frac{1}{(T_f - T_m)} = \frac{P(0)}{2} \frac{R_f}{(T_f - T_m)} \text{ and } h_m = \gamma_m \frac{(T_f - T_m)}{(T_{out} - T_{in})}.$$
(5)

### 3. LINEAR STABILITY ANALYSIS

Equations (1) are non-linear, because the reactivity is a function of time. The usual approach to this difficulty is to linearize these two equations by assuming only small reactivity and power perturbations<sup>14</sup>. Proceeding this way and substituting the Laplace transform of the linearized version of Eqs. (1) into each other, one obtains the zero-power reactivity transfer function:

$$G_6(s) \equiv \frac{\delta P(s)}{\delta \rho(s)} = \frac{P_0}{\Lambda s + \beta - \rho_0 - \sum_{i=1}^6 \frac{\beta_i \lambda_i}{s + \lambda_i}} = \frac{P_0}{\Lambda s - \rho_0 + \sum_{i=1}^6 \frac{\beta_i s}{s + \lambda_i}} \quad (6)$$

Assuming a critical reactor ( $\rho_0=0$ ) and only one group of delayed neutrons, this equation simplifies to:

$$G_1(s) \equiv \frac{\delta P(s)}{\delta \rho(s)} = \frac{P_0(s + \lambda)}{\Lambda s(s + \lambda + \frac{\beta}{\Lambda})} \quad (7)$$

Figure 2 shows the magnitude and phase of both  $G_6(s)$  and  $G_1(s)$  for a PWR fuelled with  $\text{UO}_2$  and with MF=2. In fact, these plots show the magnitude and phase of the power response to a sinusoidal reactivity perturbation as a function of frequency when feedback effects are neglected.

Assume  $\delta T_m \ll \delta T_f$  in the first of Eqs. (2), the Laplace transforms of Eqs. (2) yield the feedback reactivity transfer functions of the fuel and moderator:

$$H_f(s) \equiv \frac{\delta T_f(s)}{\delta P(s)} = \frac{C_f^{-1}}{s + \gamma_f} \quad (8)$$

and:

$$H_m(s) \equiv \frac{\delta T_m(s)}{\delta T_f(s)} = \frac{\gamma_m}{s + \gamma_m + 2h_M} = \frac{\gamma_m}{s + f_m}.$$

Note that in this model the fuel feedback transfer function relates fuel temperature to power, while the moderator feedback transfer function relates moderator temperature to fuel temperature. Of course, in reality, there is also a direct heating component of the moderator by means of energy deposition of gamma rays and neutrons in the moderator, but this effect is usually only a few percent of the total heating and is neglected in this analysis.

The combined reactivity feedback transfer function writes:

$$H(s) = \alpha_f H_f(s) \left( 1 + \frac{\alpha_m}{\alpha_f} H_m(s) \right), \quad (9)$$

where  $\alpha_f$  and  $\alpha_m$  are the fuel and moderator temperature coefficients of reactivity, respectively. In this analysis, the feedback reactivity is subtracted from the externally introduced reactivity, which implies that  $\alpha_f$  and  $\alpha_m$  are positive if a temperature rise of the fuel or moderator temperature gives a negative reactivity feedback (negative feedback convention<sup>14</sup>).

The open loop transfer function then reads:

$$G(s)H(s) = KF(s) = \frac{\alpha_f P_0}{C_f \Lambda} \frac{(s + \lambda)(s + t_m)}{s \left( s + \lambda + \frac{\beta}{\Lambda} \right) (s + \gamma_f)(s + f_m)} \quad (10)$$

with inverse time constants:

$$t_m = f_m + \frac{\alpha_m}{\alpha_f} \gamma_m; \lambda + \frac{\beta}{\Lambda} \approx \frac{\beta}{\Lambda}; \gamma_f = \frac{h_s A_f}{C_f}; f_m = \gamma_m + 2h_m = 2\gamma_m \frac{(T_f - T_{in})}{(T_{out} - T_{in})}. \quad (11)$$

It is seen that the open-loop transfer function has two zeroes and four poles. Furthermore, the gain  $K = \alpha_f P / C_f \Lambda$  is inversely proportional to the generation time  $\Lambda$ , which means that it is very sensitive to the fuel type and MF ratio. The frequency response of the open-loop transfer function is shown in Fig. 3 for UO<sub>2</sub> fuel and for MOX fuels with the MF ratio as a parameter. This transfer function differs considerably from the zero-power transfer function shown in Fig. 2 due to the fuel and moderator feedback mechanisms. Especially for high frequencies (>1 Hz), the open-loop transfer function has a lower magnitude and a stronger negative phase shift. However, the differences between the fuels are very small.

The root-locus plot is obtained by solving  $KF(s) = -1$  for  $s = \sigma + j\omega$  with  $K$  as a parameter that increases from zero to infinity. This follows from the closed-loop transfer function:

$$Y(s) = \frac{G(s)}{1 + G(s)H(s)} = \frac{G(s)}{1 + KF(s)} \quad (12)$$

that becomes infinity for above-mentioned condition. For all fuel types used (UO<sub>2</sub> and MOX with different MF ratios), the root-locus plot is schematically shown in Fig. 4. The loci start at the poles  $P$  and end at the zeroes  $Z$  of the open loop transfer function  $G(s)H(s)$  given by Eq. (10). When the loci leave the  $\sigma$ -axis, oscillatory behaviour occurs. The values of the gain, poles and zeroes calculated by:

$$K = \frac{\alpha_f P_0}{C_f \Lambda}; P_2 = -\gamma_f; P_3 = -f_m; P_4 = -\lambda - \frac{\beta}{\Lambda}; Z_1 = -\lambda; Z_2 = -t_m, \quad (13)$$

are given in Table I for different fuels and MF ratios. Clearly the gain  $K$  and the pole  $P_4$  are very sensitive to the fuel and the MF ratio due to  $\Lambda$ , while the poles  $P_2$  and  $P_3$  and the zero  $Z_2$ , are mainly sensitive to the MF ratio by the factors  $A_f$ ,  $A_m$  and  $C_m$  in Eq. (3). It is noted that both  $K$  and  $P_4$  are not sensitive to  $\Lambda$  when the prompt-jump approximation is used<sup>14</sup>.

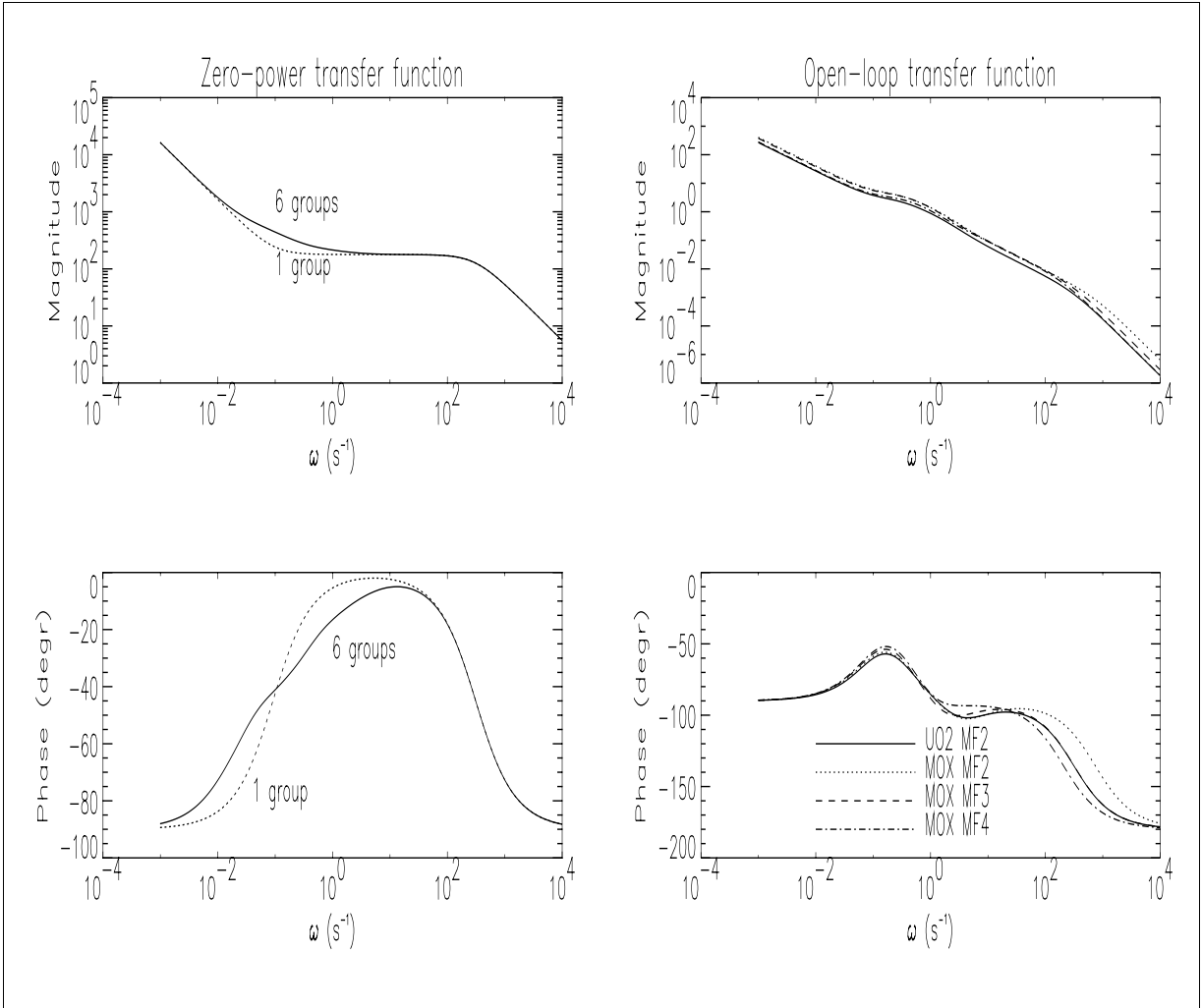


Figure 2: Zero-power transfer function  $G(s)/P_0$  for a standard UO<sub>2</sub> fuelled PWR with the number of delayed neutron groups as a parameter.

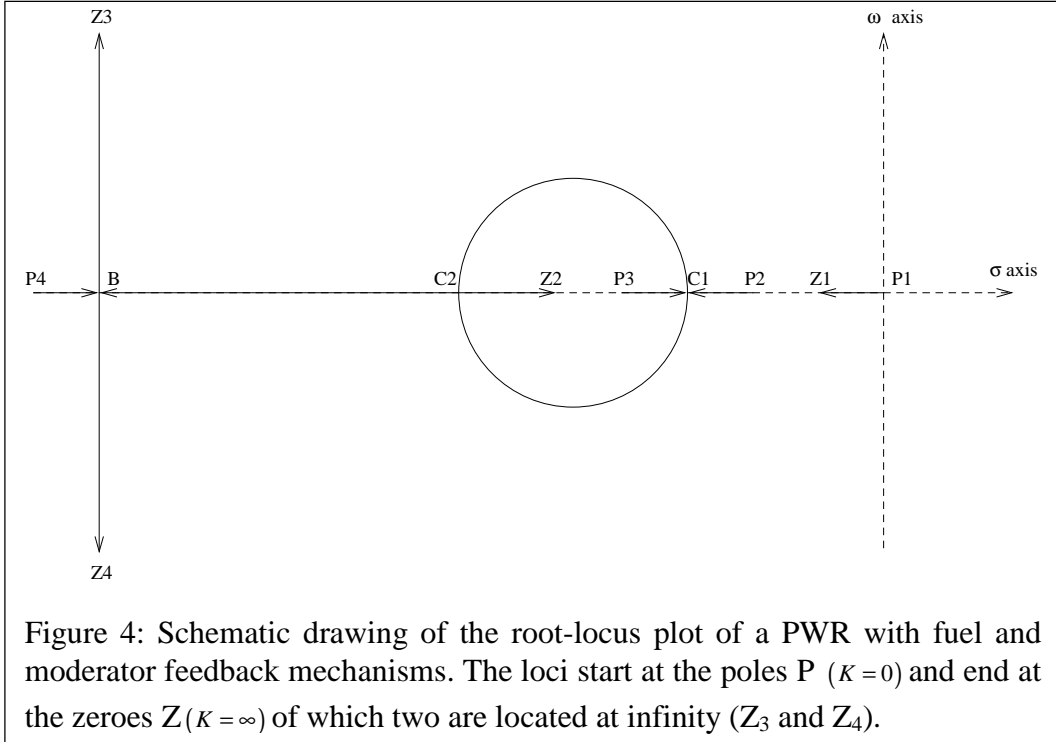
Figure 3: Open-loop transfer function  $G(s)H(s)$  (Eq. 10) for PWRs with different fuels and MF ratios. One delayed neutron group was used.

Once the roots have been determined, the time-dependent behaviour of the reactor upon external reactivity input can be calculated by the inverse Laplace transform of  $Y(s)$  given by Eq. (12). The solution is a sum of weighted exponentials:

$$y(t) = \sum_{i=1}^4 A_i \exp(s_i t), \quad (14)$$

where the  $s_i$  are the values of  $s = \sigma + j\omega$  given by the root-locus plot for the given value of the gain  $K$ . It is undesirable that the loci in Fig. 4 cross the  $\omega$ -axis into the right half plane with positive  $\sigma$ -value, because the reactor power would continuously increase after an externally introduced reactivity. This is the unstable region for reactor operation.





It should be noted here that the amplitudes in Eq. (14) spread several orders of magnitude, because the poles of the transfer function  $Y(s)$  in Eq. (12) differ so much. Table I shows that the poles spread several orders of magnitude, with the result that  $A_4$  equals about unity for all fuels and that this amplitude is a factor of one thousand larger than the others. Consequently, the pole  $P_4$  dominates the time-dependent behaviour of the reactor after a small external disturbance, that is to say, within the limit of linear stability analysis.

As mentioned before, the  $\sigma$ -values determine the exponentially increasing or decreasing trend of the reactor power after an externally introduced reactivity, while the  $\omega$ -values “merely” determine the oscillatory behaviour superimposed on this trend. Because we are interested in the first, we will focus in the remainder of this section on the  $\sigma$ -values rather than the  $\omega$ -values. Therefore, instead of showing the root-loci in the  $(\sigma, \omega)$  plane, it is more illustrative to show the  $\sigma$ -values as a function of the gain. This is done in Fig. 5 for  $UO_2$  fuel with  $MF=2$  and for MOX fuel with  $MF=2$  and  $MF=3$ , and in Fig. 6 for MOX fuel made of four times recycled plutonium. Note that in these figures, the loci starting in poles  $P_2$  and  $P_3$  coincide between  $C_1$  and  $C_2$  where the two roots are each others complex conjugate (see Fig. 4). The locus of  $P_2$  ends in  $Z_2$ , while the locus of  $P_3$  meets that of  $P_4$  in point  $B$ . With increasing gain  $K$ , the roots of the loci of  $P_3$  and  $P_4$  are also complex conjugates of each other.

In each of these plots, the crossing of the dotted line and the  $\sigma$ -curves between  $P_1$  and  $Z_1$  occur at the same position ( $\sigma = 0.07 \text{ s}^{-1}$ ), which indicates that the (very) long-term trend determined by the decay of the neutron precursors is the same for all fuels and all MF ratios. Apparently, all fuels have about the same value for  $\lambda$  in Eq. (10). The crossing of the dotted line and the  $\sigma$ -curve between  $P_4$  and  $B$  is the same for  $UO_2$  fuel and for MOX with  $MF=3$ , but

is larger for MOX fuel with MF=2. This is mainly due to pole  $P4$  that equals  $\beta/\Lambda$  in value. Compared with  $UO_2$  fuel,  $\beta$  reduces for MOX fuel due to the small delayed neutron fraction of  $^{239}\text{Pu}$ , but the neutron generation time decreases even more. To illustrate this,  $\beta$  decreases from 0.56% for  $UO_2$  to 0.39% for MOX with MF=2, while  $\Lambda$  decreases from 18 to  $5.3\mu\text{s}$ . For MOX fuel with MF=3,  $\Lambda$  equals  $12\mu\text{s}$  (see Refs. 11 and 12).

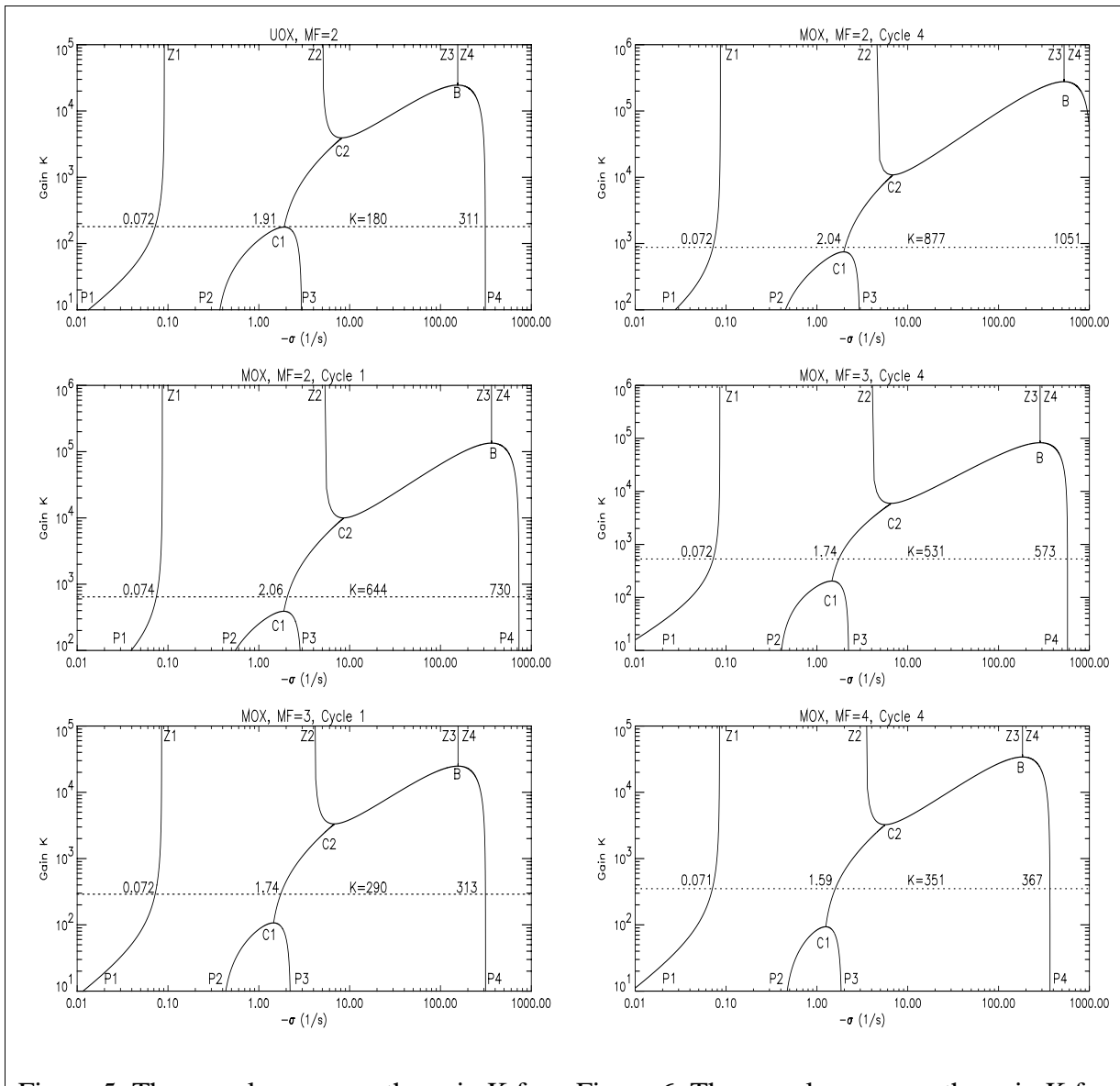


Figure 5: The  $\sigma$ -values versus the gain  $K$  for different PWR fuels. The dotted horizontal lines show the gain at nominal operation, and the values shown are the  $\sigma$ -values at the crossings. The loci start at the poles  $P$  ( $K=0$ ) and end at the zeroes  $Z$  ( $K=\infty$ ).

Figure 6: The  $\sigma$ -values versus the gain  $K$  for MOX fuels. The dotted horizontal lines show the gain at nominal operation, and the values shown are the  $\sigma$ -values at the crossings. The loci start at the poles  $P$  ( $K=0$ ) and end at the zeroes  $Z$  ( $K=\infty$ ).

The  $\sigma$ -value at the crossing of the dotted line and the curve between  $C1$  and  $C2$  for  $UO_2$  fuel ( $\sigma=1.91s^{-1}$ ) is between the values of MOX fuel with  $MF=2$  ( $\sigma=2.06s^{-1}$ ) and MOX fuel with  $MF=3$  ( $\sigma=1.74s^{-1}$ ). With decreasing fuel pin radius (increasing MF ratio), two trends with opposite sign can be observed. First, the heat capacity of the fuel decreases due to the smaller fuel volume, which shifts  $P2$  to a larger negative value proportional with the inverse of the fuel pin radius (to the right in Figs. 5 and 6). Secondly, the heat capacity of the moderator increases, which shifts  $P3$  to smaller negative values (to the left in Figs. 5 and 6).

Table I: Values of the gain and the poles and zeroes for a PWR with different fuels and MF ratios. The formulas are given by Eq. (12). The poles and zeroes are given in units of  $s^{-1}$ .

Reactor	$UO_2$	MOX	MOX	MOX
MF ratio	2	2	3	4
Gain K	180	644	290	184
Pole P1	0	0	0	0
Pole P2	-0.33	-0.33	-0.38	-0.42
Pole P3	-2.97	-2.97	-2.24	-1.87
Pole P4	-311	-731	-313	-204
Zero Z1	-0.091	-0.087	-0.085	-0.084
Zero Z2	-4.99	-5.20	-4.08	-2.93

In Fig. 6, the same plots are given for MOX fuel with different MF ratios after four times plutonium recycling. Again, the crossing between the dotted line and the  $\sigma$ -curve between  $P1$  and  $Z1$  is at  $\sigma=0.07s^{-1}$ . Between  $C1$  and  $C2$ , the dotted line crosses the  $\sigma$ -curves at values of  $\sigma=2.0s^{-1}$  for  $MF=2$ , at  $\sigma=1.7s^{-1}$  for  $MF=3$  and at  $\sigma=1.6s^{-1}$  for  $MF=4$ . However, the clearest and most important distinction between the three pictures of Fig. 6 is the crossing between points  $P4$  and  $B$  of the dotted line with the  $\sigma$ -curves. This crossing shifts to lower values when the MF ratio increases, due to the large increase of the neutron generation time from  $3.6\mu s$  for  $MF=2$  to  $13\mu s$  for  $MF=4$ . From Figs. 5 and 6 can be concluded that for a MOX-fuelled reactor to behave like a  $UO_2$  fuelled one, the MF ratio should be three for the first recycling of plutonium, and about four for the fourth recycling (when degraded plutonium is being recycled).

#### 4. QUASI-STATIONARY APPROACH

In the quasi-stationary approach, a technique that has been used to assess the safety of innovative fast reactors<sup>15</sup>, the stationary state of the reactor after the accident is calculated by assuming that the introduced reactivity is completely compensated by the reactivity feedback mechanisms. As will be shown in the next section, the new stationary state after

the accident is reached rather soon; in most cases already within ten seconds, which justifies the approach to omit any effects due to Xenon or decay heat. The reactivity of the reactor is given by:

$$\rho = A(\tilde{P} - 1) + B\left(\frac{\tilde{P}}{\tilde{F}} - 1\right) + C(\tilde{T}_{in} - 1) + \rho_{ext}, \quad (15)$$

where  $\tilde{P}$  is the normalised power,  $\tilde{F}$  the normalised coolant flow and  $\tilde{T}_{in}$  the normalised increase of the coolant inlet temperature (for example, for a PWR with the coolant inlet temperature at 583K, the nominal inlet temperature at 573K and the environment at 293K,  $\tilde{T}_{in} = (583 - 293) / (573 - 293) = 1.0357$ ). With these definitions,  $C$  equals the temperature defect (the reactivity needed to go from cold zero power to hot zero power),  $B$  equals the power/flow coefficient, and  $A$  equals the power defect (the reactivity needed to go from hot zero power to hot full power without any effect due to Xenon). These three coefficients are negative and equal to:

$$A = -\alpha_f \Delta T_f; \quad B = -(\alpha_f + \alpha_m) \frac{\Delta T_C}{2}; \quad C = -(\alpha_f + \alpha_m) \Delta T_{in}. \quad (16)$$

Here  $\Delta T_f$  is the fuel temperature from hot zero power to hot full power,  $\Delta T_C$  is the coolant temperature rise between inlet and outlet, and  $\Delta T_{in}$  is the inlet temperature rise from cold zero power to hot zero power. The minus signs in Eq. (16) are needed to compensate for the fact that the  $\alpha_f$  and  $\alpha_m$  are positive when a temperature rise gives a negative reactivity introduction (negative feedback convention<sup>14</sup>).

Typical PWR transients are described in Ref. 16. The first transient considered in this paper, is a malfunctioning of the reactivity control system, leading to a sudden introduction of reactivity (RIA). Other transients concern a malfunctioning of the reactor coolant system, like a reduction of coolant flow (LOF) or an increase of coolant flow (POS). Two other transients concern an increase of feed water temperature (LOHS), or a decrease of feed water temperature (MCA).

#### 4.1 REACTIVITY INDUCED ACCIDENTS (RIA)

Due to control rod withdrawal, for example, external reactivity is introduced that is compensated by an increase of reactor power  $\tilde{P} \uparrow$ . At first instance,  $\tilde{T}_{in} = 1$  and  $\tilde{F} = 1$ . Then Eq. (15) gives  $\tilde{P} = 1 - \rho_{ext} / (A + B)$ . To limit this reactor power surge,  $(A + B)$  should be large negative. Because of the large reactor power and the constant heat removal in the secondary circuit, after some time the coolant inlet temperature will rise  $\tilde{T}_{in} \uparrow$ , which introduces a negative reactivity that shuts down the reactor. At the end  $\tilde{P} = 1$ ,  $\tilde{F} = 1$  and  $\tilde{T}_{in} = 1 - \rho_{ext} / C$ . To limit the inlet temperature,  $C$  should be large negative.

#### 4.2 LOSS OF FLOW WITHOUT SCRAM (LOF)

In this case, the coolant flow reduces  $\tilde{F} \downarrow$  while  $\tilde{T}_{in} = 1$ . This causes an increase of coolant outlet temperature and a decrease of reactor power. The reactor stabilises at  $\tilde{P} / \tilde{F} = 1 + A / B$ . To limit the consequences of this transient,  $A$  should be small negative and  $B$  large negative.

#### 4.3 PUMP OVERSPEED (POS)

In this transient, the coolant flow increases  $\tilde{F} \uparrow$  with constant inlet temperature ( $\tilde{T}_in = 1$ ). The reactor power increases to compensate for the lower temperature rise of the coolant during passage in the core. The maximum power, which is determined by  $\tilde{P} = (A+B)/(A+B/\tilde{F})$ , can be limited when  $A$  is large negative and  $B$  small negative. After some time, the larger power leads to an increase of the inlet temperature until  $\tilde{T}_in = 1 + (B/C)(1 - 1/\tilde{F})$ . To limit this  $\tilde{T}_in$ ,  $B$  should be small negative and  $C$  large negative. However, from Eq. (16) can be seen that the ratio of  $B$  and  $C$  can only be varied by changing  $\Delta T_c$  and/or  $\Delta T_in$ .

#### 4.4 LOSS OF HEAT SINK (LOHS)

In this scenario, the inlet temperature rises  $\tilde{T}_in \uparrow$  with constant coolant flow  $\tilde{F} = 1$ . Then the reactor power decreases, because  $C < 0$ . At the end,  $\tilde{P} = 0$  and the inlet temperature becomes  $\tilde{T}_in = 1 + (A+B)/C$ . To limit the consequences of this scenario,  $(A+B)$  should be small negative, and  $C$  should be large negative.

#### 4.5 MODERATOR COOLING ACCIDENT (MCA)

In this scenario, the cooling capacity increases, e.g. due to a steam line rupture, which implies that the inlet temperature decreases  $\tilde{T}_in \downarrow$  with constant flow  $\tilde{F} = 1$ . The reactor power increases to a stationary value  $\tilde{P} = 1 + C(1 - \tilde{T}_in)/(A+B)$ . To limit the reactor power,  $C$  should be small negative and  $(A+B)$  large negative.

The values of  $A$ ,  $B$  and  $C$  are given in Table III for UO<sub>2</sub> fuel and for MOX fuel with various MF ratios. The coefficient  $A$  is proportional to the Doppler coefficient that is, compared with UO<sub>2</sub> fuel, about 5% larger for MOX fuel with MF=2 and 20% lower for MOX fuel with MF=4. The moderator temperature coefficient follows the same trend, but with larger differences. Compared with UO<sub>2</sub>, the MTC is 15% stronger negative for MOX fuel with MF=2, and about 30% less negative for MOX fuel with MF=4. Therefore, the values of  $B$  and  $C$  vary over a wider range. For each accident, Table IV shows the MF ratio for MOX-fuelled PWRs giving the lowest impact and highest impact. The differences between the best and worst MF ratio generally range up to several tens of percents, except for the POS scenario where it reaches only 3% at the maximum. That is because the ratio of  $B$  and  $C$  is constant, and  $(A+B)/(A+B/\tilde{F})$  is almost not dependent on the MF ratio.

For each transient, Table IV shows the MF ratio that gives the lowest and highest impact, respectively. The impact factor given in this table is relative to that of standard UO<sub>2</sub> fuel. For the RIA, LOF and LOHS transients, an MF ratio of 2.5 has preference, while for the MCA transient, a large value of MF=4 gives the lowest impact. The POS transient is not sensitive to the MF ratio at all. When degraded plutonium is used, like that used during the fourth recycling (see Table V), it is advantageous for the MCA transient to use an MF ratio of two, while for the RIA, LOF and LOHS transients, an MF ratio of about three has preference.

Table II: Limits and demands for A, B and C for different transients.

Scenario	Limits	Demands
RIA	$\tilde{P} = 1 - \frac{\rho_{ext}}{A+B}; \tilde{T}_{in} = 1 - \frac{\rho_{ext}}{C}$	(A+B) large negative C large negative
LOF	$\frac{\tilde{P}}{\tilde{F}} = 1 + \frac{A}{B}$	A small negative B large negative
POS	$\tilde{P} = \frac{A+B}{A+B/\tilde{F}}; \tilde{T}_{in} = 1 + \frac{B}{C}(1 - \frac{1}{\tilde{F}})$	A large negative B small negative C large negative
LOHS	$\tilde{T}_{in} = 1 + \frac{A+B}{C}$	(A+B) small negative C large negative
MCA	$\tilde{P} = 1 + \frac{C}{A+B}(1 - \tilde{T}_{in})$	(A+B) large negative C small negative

Table III: Values of coefficients A, B and C (pcm) defined by Eq. (16).

	Fuel→	UO <sub>2</sub>	MOX	MOX	MOX
	Cycle↓	MF=2	MF=2	MF=3	MF=4
A	1	-980	-1030	-940	-820
B	1	-740	-850	-840	-520
C	1	-13700	-15800	-15600	-9600
A	4		-970	-940	-870
B	4		-520	-800	-790
C	4		-9700	-14800	-14700

Table IV: MF ratio and impact factor of MOX fuelled PWRs relative to that of UO<sub>2</sub> fuel for the **first** recycling of plutonium.

Transient scenario	Lowest impact		Highest impact	
	MF ratio	Impact (%)	MF ratio	Impact (%)
RIA	2.5	-11	4.0	+43
LOF	2.5	-20	4.0	+19
POS	4.0	-1	2.5	+3
LOHS	2.5	-11	4.0	+11
MCA	4.0	-9	2.5	+13

Table V: MF ratio and impact factor of MOX fuelled PWRs relative to that of UO<sub>2</sub> fuel for the **fourth** recycling of plutonium.

Transient scenario	Lowest impact		Highest impact	
	MF ratio	Impact (%)	MF ratio	Impact (%)
RIA	3.0	-1	2.0	+41
LOF	3.5	-16	2.0	+40
POS	2.0	-3	4.0	+2
LOHS	3.5	-10	2.0	+23
MCA	2.0	-18	3.5	+11

## 5. NUMERICAL ANALYSIS

The point-kinetics model with fuel and moderator temperature feedback described in Section 2 has been programmed in a FORTRAN code driven by a PERL script. The same accidents as described in Section 4 have been analysed for as many seconds as necessary to reach the stationary state, which of course should correspond to the results of the quasi-stationary approach. In the simulation of each scenario, the point-kinetics code was initially run for one second at nominal conditions after which the external disturbance was introduced. Table VI gives an overview of the external disturbance applied to model each accident scenario.

The RIA has been modelled by assuming that the reactivity increases instantaneously with 0.5\$, the LOHS by assuming the inlet temperature equals the outlet temperature shifted with  $\tau$  seconds (in our case  $\tau=20$ ), and the LOF by setting to zero the power removal inverse time constant  $h_m$ . The MCA has been modelled by reducing the inlet temperature with 20K and the POS by increasing the inverse time constant  $h_m$  by 50% at constant inlet temperature. Because the secondary circuit was not modelled, many effects cannot properly be accounted for. However, if the results are used for comparison only, the model assesses many interesting effects connected to nuclear reactor safety<sup>17</sup>.

Table VI: External disturbance applied in the point-kinetics FORTRAN code to model the transient. The parameter  $\tau$  in the LOHS transient is the time interval needed for the cooling water to flow through the primary circuit from the exit of the core to the inlet. In the simulations  $\tau$  is (arbitrarily) set to 20 s. The parameter  $\alpha_m$  equals the MTC.

Transient	External disturbance
RIA	$\Delta\rho = 0.5\text{\$}$
LOF	$h_m = 0$ (see Eq. (2))
POS	$\Delta h_m = 0.5h_m$ (see Eq. (2))
LOHS	$T_{in}(t) = T_{out}(t - \tau); \Delta\rho(t) = \alpha_m \Delta T_{in}(t)$
MCA	$\Delta T_{in} = -20\text{ K}; \Delta\rho = \alpha_m \Delta T_{in}$

Figure 7 shows the results for the RIA transient. The power jumps instantaneously with a factor of two, which agrees of course with the prompt jump approximation, but stabilises after a few seconds to a level 10 to 20% above nominal. The fuel temperature increases only 35K for the MOX fuels with MF=2 and MF=3, about 45K for MOX fuel with MF=4 and 55K for UO<sub>2</sub> fuel. The average coolant temperature increases only a few degrees. The temperatures of all the MOX fuels remain below that of UO<sub>2</sub> fuel. It is noted that the reactivity increase of 0.5\$ expressed in *pcm* is much less for the MOX fuels than for UO<sub>2</sub> due to the smaller  $\beta_{eff}$  (0.39% versus 0.56%).

The effects of the LOF transient are rather moderate (Fig. 8). Due to the increase of the coolant temperature, power levels off to zero. For each reactor, the fuel and coolant temperatures reach eventually the same value of 730K for UO<sub>2</sub>, 715K for MOX fuel with MF=2, and about 695K for MOX fuels with MF=3 and MF=4. Again the temperatures of all the MOX fuels are lower than that of the UO<sub>2</sub> fuel, and much lower than any limit imposed by cladding interactions ( $\approx$ 1475K).

In the POS transient (see Fig. 9), power increases within one second to a level of 25% above nominal for the MOX fuel with MF=4, and 65% above nominal for MOX with MF=2. Already after three seconds, power stabilises for all fuels at a level 15% above nominal. The fuel temperature increases 50K for UO<sub>2</sub>, 45K for MOX with MF=4, and 55K for MOX with MF=2. The average coolant temperature decreases 4K for all fuels.

The LOHS transient is modelled by assuming that the inlet temperature equals the outlet temperature shifted  $\tau$  seconds in time (in our case 20 seconds is assumed, but in reality this value might be larger). Results are shown in Fig. 10. For all fuels, the fuel temperature decreases about 300K, while the moderator temperature increases 40K. The oscillatory behaviour is due to the circulation time of the coolant. The average moderator temperatures of the MOX fuels with MF=2 and MF=3 are slightly lower than that of the other two fuels.

The most penalising transient for the utilisation of MOX fuel in PWRs is probably the MCA or cold water ingress scenario<sup>8</sup>. For a 20K reduction of the inlet temperature, results are shown in Fig. 11 for the first recycling of plutonium and in Fig. 12 for the fourth recycling. During the first plutonium recycling, both the MOX fuels with MF=2 and MF=3 become prompt supercritical, while the UO<sub>2</sub> fuel and the MOX with MF=4 remain sub-critical. During the fourth recycling, the MOX fuels with MF=3 and MF=4 become prompt supercritical, while the MOX with MF=2 remains sub-critical. For the prompt super-critical fuels, a large power spike is seen, as well as an instantaneous increase of fuel temperature. For the sub-critical fuels, the fuel temperature increases more gradually. The total increase of the average fuel temperature is between 150 and 200K.

## CONCLUSIONS

When plutonium is to be recycled in a PWR, the MF ratio can be adapted to influence the fuel and moderator temperature reactivity coefficients, and the kinetic parameters like the mean



neutron generation time. Doing this, the dynamic behaviour of the reactor will change accordingly. In this paper, this behaviour has been investigated from three viewpoints:

- Linear stability analysis for small perturbations around the working point of the reactor.
- Quasi-stationary approach to assess the ‘critical’ parameters after a specific transient.
- Numerical analysis to assess the ‘critical’ parameters during a transient.

From the linear stability analysis described in Section 3, it can be concluded that the pole of the closed-loop transfer function that is most negative, dominates the time-dependent behaviour of the reactor upon small external reactivity disturbances. The ratio of the effective delayed neutron fraction and the mean neutron generation time of the fuel dominates the  $\sigma$ -value of that pole that determines the exponentially decaying response of the reactor. For a MOX-fuelled reactor to behave like an UO<sub>2</sub>-fuelled reactor, the MF ratio should be three for plutonium during the first recycling, and about four for plutonium during the fourth recycling (see Figs. 5 and 6).

From the quasi-stationary analysis, the impact on power and temperature is calculated for five scenarios. For transients connected to an instantaneous increase of reactivity (RIA), a reduction of coolant flow (LOF), or an increase of coolant inlet temperature (LOHS), an MF ratio of 2.5 has the lowest impact on power and/or temperatures (see Table IV). For transients connected with a decrease of coolant inlet temperature (MCA), a high MF ratio of four has preference. Transients connected to an increase of coolant flow (POS) are rather insensitive to the MF ratio used. When degraded plutonium is recycled, as is the case during the fourth recycling (see Table V), an MF ratio of three has preference for the RIA, LOF and LOHS transients, while an MF ratio as low as two has preference for the MCA transient.

Figure 7 shows that all MOX fuels behave better during a RIA transient, because of the stronger negative reactivity feedback coefficients (at least when the fuel temperature feedback coefficient is expressed in units of  $\beta_{eff}$ ). The same conclusion holds for the LOF and LOHS transients. During the POS transient, the power surge for MOX fuel with MF=2 is larger than that of UO<sub>2</sub> fuel, due to the stronger negative moderator temperature coefficient. The MOX fuel with MF=4 leads to a smaller power surge and lower temperatures. During the MCA transient, simulated by a 20K decrease of coolant inlet temperature, the MOX fuels with MF=2 and MF=3 become prompt supercritical leading to a large power spike at the beginning of the transient (see Fig. 11). In this case, an MF ratio of 4 has preference. When recycling degraded plutonium, the MOX fuels with MF=3 and MF=4 become prompt critical (see Fig. 12), and a ratio of two has preference.

## REFERENCES

- 1 G.J.Schlosser, W.D.Krebs, and P.Urban, "Experience in PWR and BWR Mixed-Oxide Fuel Management", *Nuclear Technology*, **102**, pp. 54-67 (1993).
- 2 F.Burtak, L.Hetzelt, and W.Stach, "Advanced Mixed-Oxide Fuel Assemblies with Higher Plutonium Contents for Pressurized Water Reactors", *Nuclear Engineering and Design*, **162**, pp. 159-165 (1996).

- 3 J.Bergeron, R.Lenain, and S.Loubiere, "100% Plutonium Recycling Feasibility in a 900 MWe PWR Core", Proceedings of International Conference on the Physics of Reactors (PHYSOR'90), Marseille, France, pp. VI-1-VI-10, (1990).
- 4 P.Barbrault, "A Plutonium-Fueled High-Moderated Pressurized Water Reactor for the Next Century", *Nuclear Science and Engineering*, **122**, pp. 240-246 (1996).
- 5 A.Puill and J.Bergeron, "Advanced Plutonium Fuel Assembly: An Advanced Concept for Using Plutonium in Pressurized Water Reactors", *Nuclear Technology*, **119**, pp. 123-140 (1997).
- 6 U.Kasemeyer, J.M.Paratte, P.Grimm, and R.Chawla, "Comparison of Pressurized Water Reactor Core Characteristics for 100% Plutonium-containing Loadings", *Nuclear Technology*, **122**, pp. 52-63 (1998).
- 7 H.W.Wiese, "Investigation of the Nuclear Inventories of High-Exposure PWR Mixed-Oxide Fuels with Multiple Recycling of Self-Generated Plutonium", *Nuclear Technology*, **102**, pp. 68-80 (1993).
- 8 S.Aniel-Buchheit, A.Puill, and R.Sanchez, "Plutonium recycling in a Full-MOX 900 MWe PWR: Physical Analysis of Accident Behaviors", *Nuclear Technology*, **128**, pp. 245-255 (1999).
- 9 S.E.Corno, M.L.Buzano, and P.Ravetto, "A Rigorous Mathematical Technique for Reactor Dynamics: Application to Safe Plutonium Recycling", *Nuclear Science and Engineering*, **105**, pp. 142-159 (1990).
- 10 J.L.Kloosterman, J.C.Kuijper, and P.F.A.de Leege, "The OCTOPUS Burnup and Criticality Code System", Proceedings of International Conference on the Physics of Reactors (PHYSOR'96), Mito, Japan, Vol. 1, pp. B-63-B-72, (1996).
- 11 J.L.Kloosterman, "Reactor Physics Aspects of Plutonium Recycling in PWRs", Proceedings of International Conference on the Physics of Nuclear Science and Technology, Long Island, New York, USA, Vol. 1, pp. 127-134, (1998).
- 12 J.L.Kloosterman and E.E.Bende, "Plutonium Recycling in PWRs: Influence of the Moderator-to-Fuel Ratio", *Nuclear Technology*, To be published (2000).
- 13 J.J.Duderstadt and L.J.Hamilton, *Nuclear Reactor Analysis*, John Wiley&Sons, Inc. (1976).
- 14 D.L.Hetrick, *Dynamics of Nuclear Reactors*, American Nuclear Society (1993).
- 15 A.J.Janssen, "On the Safety of the ALMR", Report ECN-R--94-011, ECN, Petten, Netherlands, (1994).
- 16 B.Pershagen, *Light Water Reactor Safety*, Pergamon Press (1989).
- 17 H.van Dam, "Physics of Nuclear Reactor Safety", *Reports on Progress in Physics*, **11**, pp. 2025-2077 (1992).

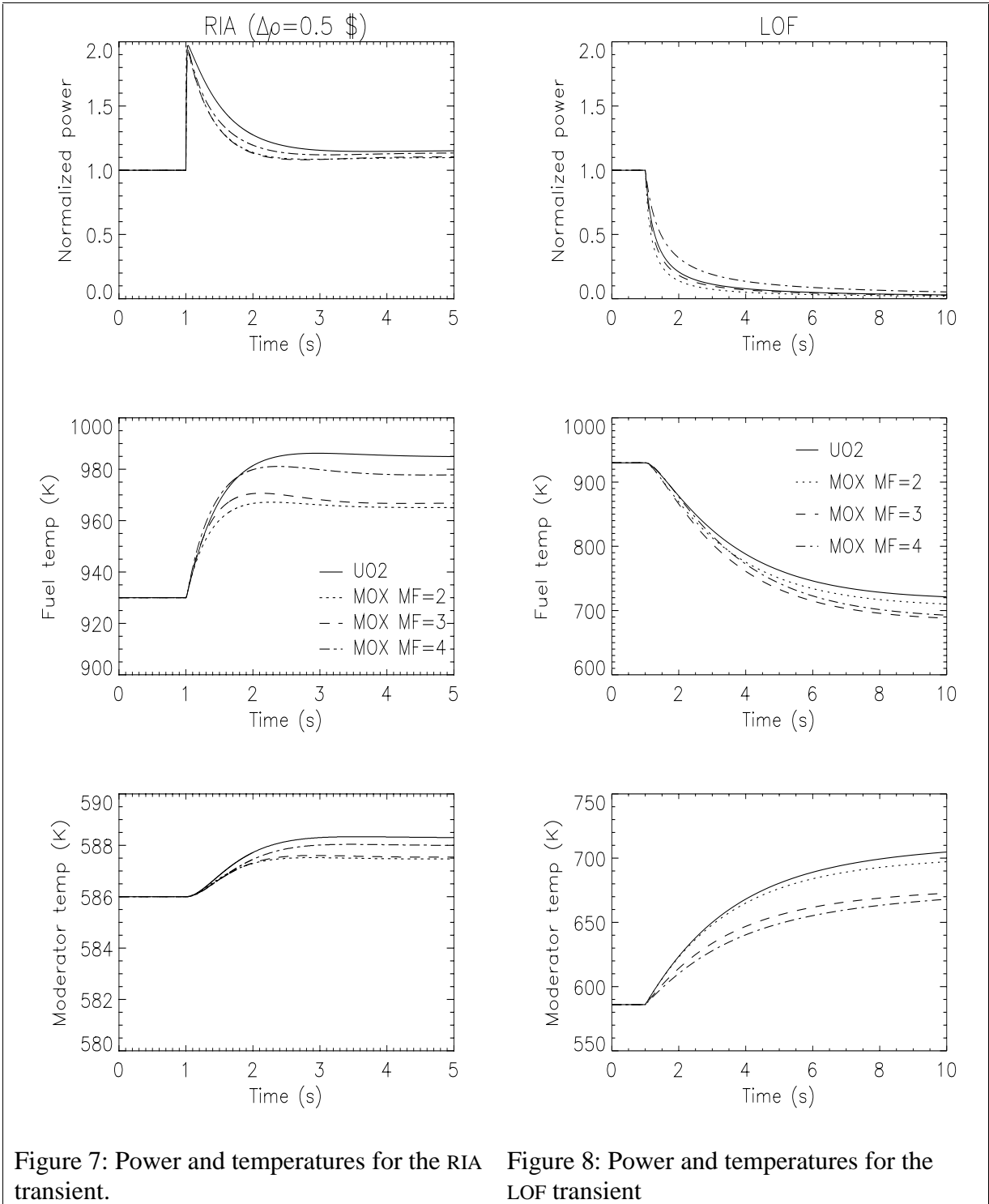


Figure 7: Power and temperatures for the RIA transient.

Figure 8: Power and temperatures for the LOF transient

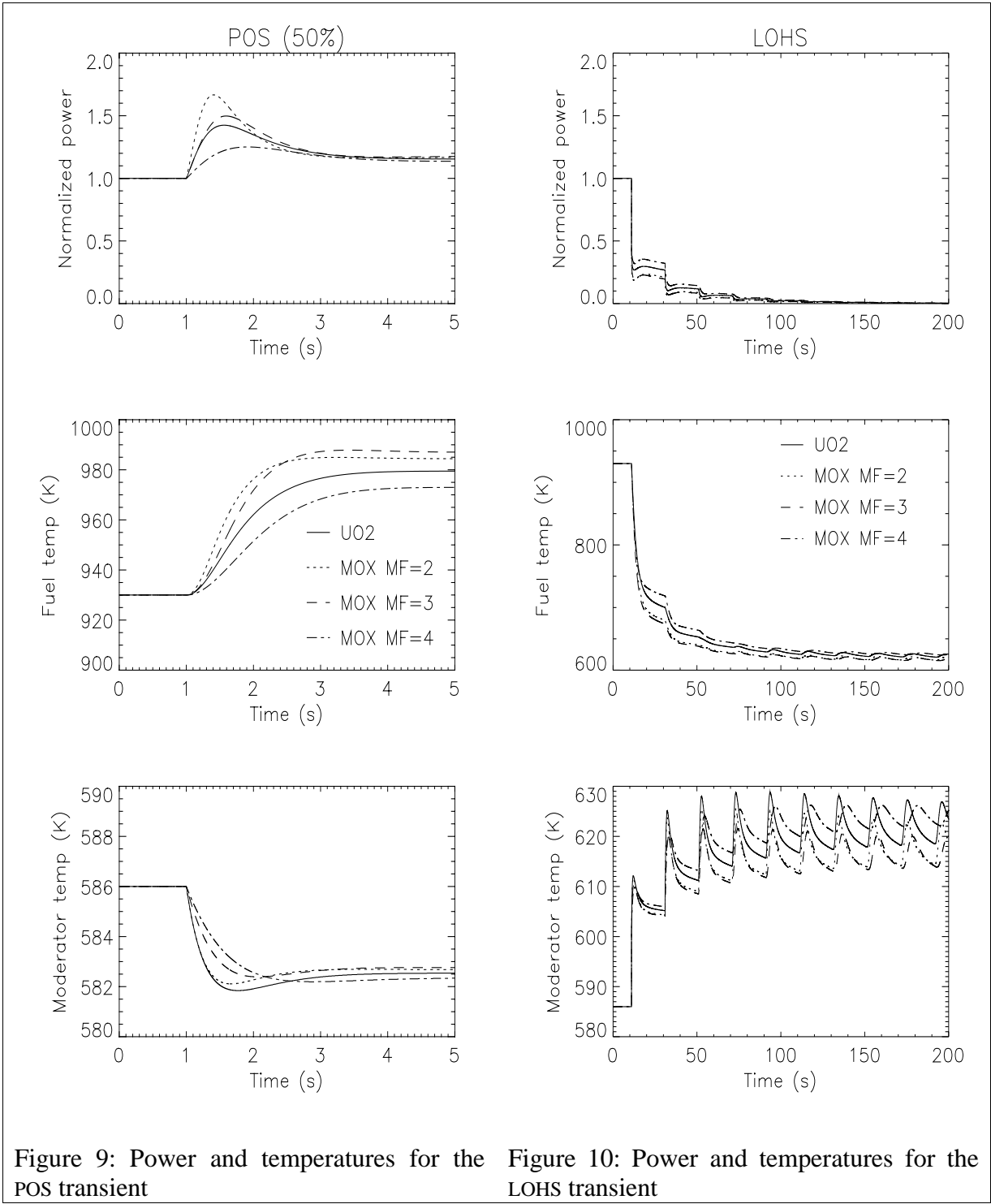


Figure 9: Power and temperatures for the POS transient

Figure 10: Power and temperatures for the LOHS transient

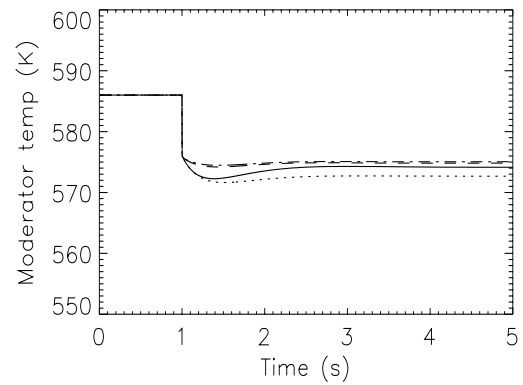
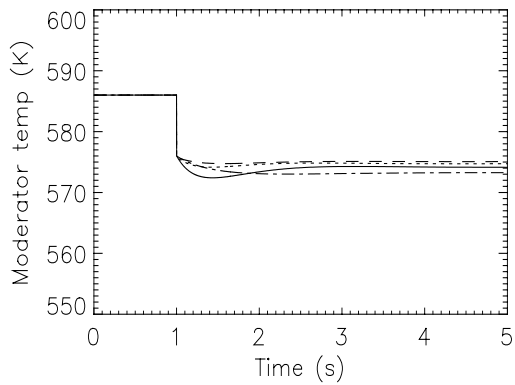
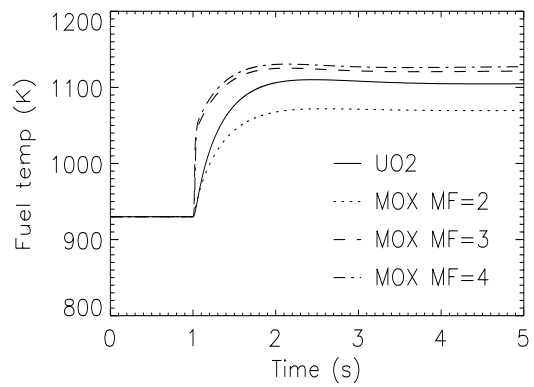
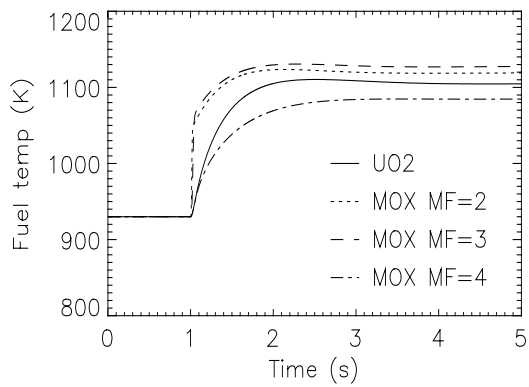
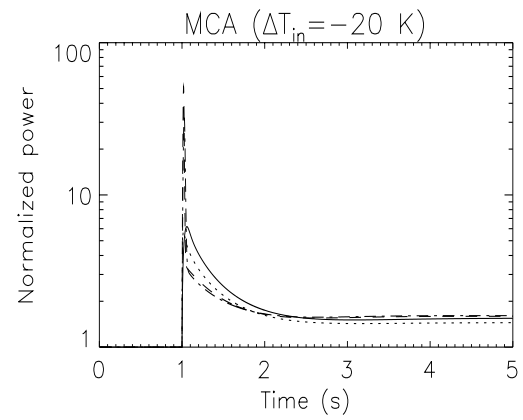
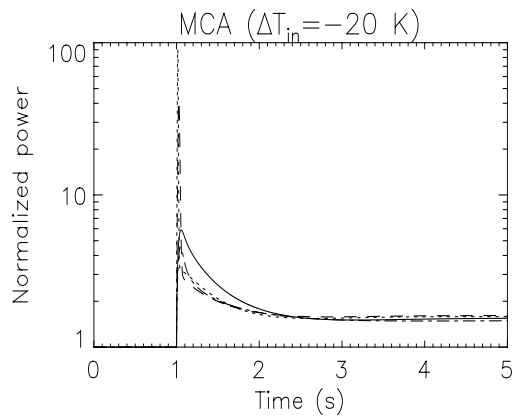


Figure 11: Power and temperatures for the MCA transient during the **first** plutonium recycling.

Figure 12: Power and temperatures for the MCA transient during the **fourth** plutonium recycling